J. Meas. Sci. Instrum., 2025, 16(2): 302-312. http://jmsi.publish.founderss.cn
DOI: 10.62756/jmsi.1674-8042.2025029 jmsi@nuc.edu.cn

Prediction of turned surface roughness based on GADF of multi-channel signal fusion and MA-ResNet

SHI Lichen*, LIU Tengfei, WANG Haitao

College of Mechanical and Electrical Engineering, Xi'an University of Architecture and Technology, Xi'an 710055, China

***Corresponding author:** SHI Lichen (shilichen20231@163.com)

Received: February 1, 2024 **Revised:** March 20, 2024 **Accepted:** May 10, 2024

Abstract: In order to achieve high precision online prediction of surface roughness during turning process and improve cutting quality, a prediction method of turned surface roughness based on Gramian angular difference field (GADF) of multi-channel signal fusion and multi-scale attention residual network (MA-ResNet) was proposed. Firstly, the multi-channel vibration signals were subdivided into various frequency bands using wavelet packet decomposition, and the sensitive channels were selected for signal fusion by doing correlation analysis between the signals of various frequency bands and the surface roughness. Then the fused signals were converted into pictures using GADF image encoding. Finally, the pictures were inputted into the residual network model combining the parallel dilation convolution and attention module for training and verifying the effectiveness of the model performance. The proposed method has a root mean square error of 0.018 7, a mean absolute error of 0.014 3, and a coefficient of determination of 0.869 4 in predicting the surface roughness, which is close to the actual value. Therefore, the proposed method had good engineering significance for high-precision prediction and was conducive to on-line monitoring of surface quality during workpiece processing.

Key words: signal fusion; Gramian angular difference field; dilated convolution; residual network; roughness prediction

0 Introduction

Surface roughness, being a crucial indicator for assessing the quality of mechanical parts, significantly influences the wear resistance, fit stability, and fatigue strength of these parts[1]. With the continuous development of intelligent machining technology, the online detection and prediction of surface roughness of machined parts has become an indispensable aspect of intelligent machining process. The traditional approach of processing followed by measurement is no longer sufficient to meet the demands of intelligent processing.

Currently, the surface roughness detection methods are mainly divided into two categories. One is the direct detection method, which collects the picture of the processed workpiece through optical sensors, and uses the image processing method to get the surface roughness of the parts[2-5]. However, due to the use of cutting fluid in mechanical processing, online optical detection of surface roughness is hindered. And the other is the indirect detection method, which is based on the cutting parameters, machine parameters, and a large number of experimental data, to establish a prediction model with the surface roughness. A large number of researchers have utilized the cutting parameters in the machining process to predict the surface roughness[6-10]. But due to the complexity of the machining environment, such models do not match well with the actual situation, resulting in low prediction accuracy and the inability to predict the surface roughness in real time.

Whether it is the change of cutting parameters, tools, workpiece materials, and machine tool performance, the final impact on the surface roughness is reflected in the form of vibration. And vibration signal as a real-variable signal, is conducive to real-time prediction of roughness. Vibration signal was used as an input parameter to establish a surface roughness prediction model[11-14]. The model can realize real-time prediction of surface roughness, but such models usually use manual extraction of features in the modeling process, which will lose a large number of important features and is not conducive to high-precision surface roughness prediction. Therefore, utilizing an adaptive feature extraction method to obtain important features related to surface roughness is the key to improve the prediction accuracy.

With the development of computer technology, deep

learning combined with vibration signal method is used in the surface roughness prediction research. Lin et al.[15,16] took the original one-dimensional raw vibration signal as input and utilized the convolutional neural network to adaptively extract the features related to the surface roughness, which actualized the prediction of surface roughness. Shi et al.[17] carried out the wavelet packet decomposition of one-dimensional vibration signals, took the wavelet packet coefficients of each frequency band as input, established a ResNet prediction model, and realized the prediction of surface roughness. The prediction model demonstrates commendable accuracy in predicting surface roughness and enables real-time predictions.

However, to further enhance the accuracy of predictions, it is imperative to address the following two issues.

1) The deep learning network model fails to fully exploit the correlation information between data when utilizing one-dimensional time series signals as input, thereby limiting its potential effectiveness.

2) During high-precision machining, the vibration signal features corresponding to different surface roughnesses change weakly, and the network model should ensure that it has the ability to recognize the weak changes in features.

A novel method was proposed for predicting turning surface roughness based on GADF of multi-channel signal fusion and MA-ResNet.

We solve the problem 1) by using GADF image encoding to convert vibration signals into two-dimensional images as model input, so that the deep learning network model can make full use of relevant information among data.

In view of problem 2), firstly, the multi-channel signal is screened and reconstructed in the frequency band layer before image encoding, so that there are more features related to surface roughness in one-dimensional vibration signal. Secondly, the multi-scale attention module was introduced on the basis of residual network to ensure the complete expression of signal feature information by using multi-scale characteristics. At the same time, the important features were highlighted through the attention mechanism, so that the model could avoid the small changes in the data signal itself, and it was difficult to identify the weak differences, so as to realize the surface roughness prediction of high-precision machining.

1 Construction of surface roughness prediction model

For high-precision prediction models, input parameters and topology structure have a very important effect on the prediction accuracy of the model. On the one hand, through multi-channel signal fusion and GADF image coding, this paper not only makes the input contain more information related to surface roughness, but also enables the deep learning model to make better use of these information. On the other hand, the combination of multi-scale expansion module and residual network makes the model avoid the difficulty to identify the weak difference due to the small change of data signal itself.

The flow of turning surface roughness prediction based on GADF of multi-channel signal fusion and MA-ResNet is specifically shown in Fig. 1, which mainly contains the following five steps.

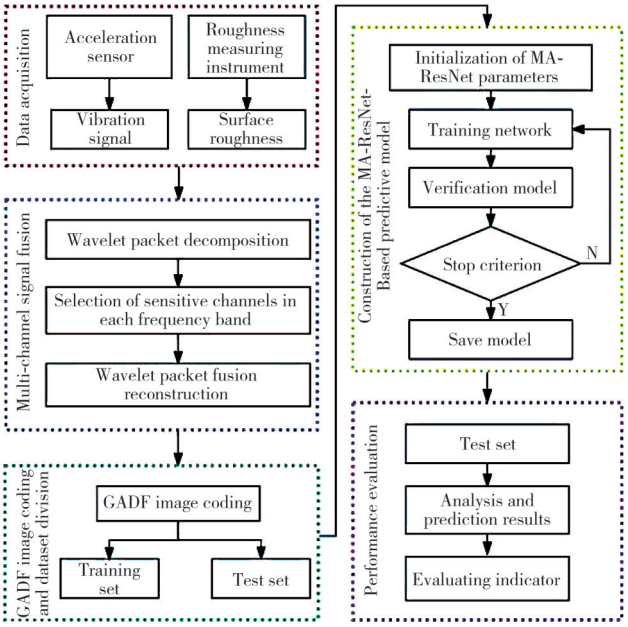

Fig. 1 Flowchart of surface roughness prediction

1.1 Multi-channel signal fusion

Multi-channel signals have richer features than single-channel signals[18], which can reflect the processing state of the measured object more completely. Because the multi-channel signals are collected at the same time, there is a certain redundancy between their signals, and the degree of influence of signals from different channels on the surface roughness is different. Therefore, how to retain the useful information related to the prediction target in the multi-channel signal and eliminate the redundant information with little relevance to the prediction target is the key to improve the prediction accuracy.

A multi-channel signal fusion method was proposed that combined wavelet packet signal segmentation and fusion reconstruction with correlation analysis. The multi-channel signal fusion process is as follows.

1) Multi-channel vibration signal acquisition.

Multiple sensors are used to collect vibration signals from different directions in the cutting system, i.e.,

$$\{X_{n,q}(k), n=1,2,3,\cdots,N; q=1,2,3,\cdots;Q, k=1,2,3,\cdots,K\}, \tag{1}$$

where n represents the sampling channel; q represents the number of samples; k represents the sampling length of the vibration signal.

2) Wavelet packet decomposition of multi-channel vibration signals. j-layer wavelet packet decomposition is carried out on multi-channel vibration signals. The wavelet packet decomposition can subdivide the signals into different frequency bands[19], which is more conducive to eliminating redundant information. The wavelet packet decomposition formula is

$$\begin{cases} p_j^{2i-1}=\sum_{k=1}^{k} h(k-2l)\,p_{j-1}^{i}(t), \\ p_j^{2i}=\sum_{k=1}^{k} g(k-2l)\,p_{j-1}^{i}(t), \end{cases} \tag{2}$$

where h represents the coefficient of high-pass filter; g represents the coefficient of low-pass filter; $p_j^i(t)$ represents the tth coefficient corresponding to the ith sub-band of the jth layer wavelet packet decomposition.

After multi-channel signal is decomposed by wavelet packet, the lowest wavelet packet decomposition coefficient $x_n^i(t)$ is obtained.

3) Selection of sensitive channels in each frequency band. The energy ratio ε_n^i of different frequency bands of each channel is calculated separately, which can represent the characteristics of vibration energy distribution. The calculation formula is

$$\varepsilon_n^i=\frac{\sum_{t=1}^{T}\left|x_n^i(t)\right|^2}{E}, \tag{3}$$

where i represents different frequency bands of the vibration signal; E represents the sum of energy of all frequency bands.

The multi-channel signal fusion flow chart is shown in Fig.2.

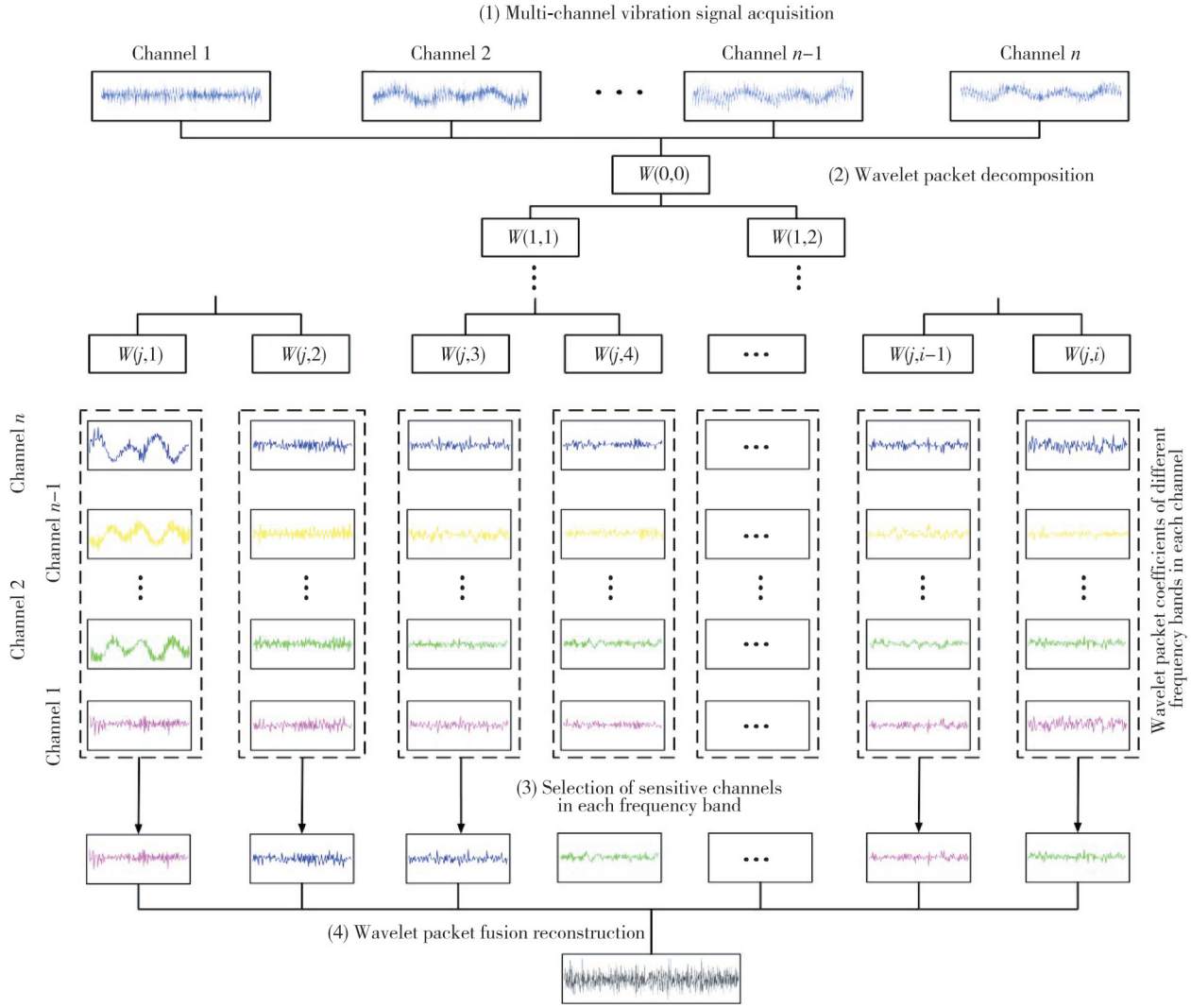

Fig. 2 Flow chart of multi-channel signal fusion

The energy proportion ε_n^i of different frequency bands in each channel is obtained. The calculation is performed for all samples, so the energy proportion $\varepsilon_n^i(q)$ of different frequency bands in each channel of all samples is obtained.

The correlation coefficient between the energy proportion of different frequency bands in each channel and the surface roughness is calculated, which is defined as the energy proportion-roughness correlation, and its calculation formula is

$$r\left\{\varepsilon_n^i(q), Ra(q)\right\}=\frac{\mathrm{Cov}\left\{\varepsilon_n^i(q)Ra(q)\right\}}{\sqrt{D\left\{\varepsilon_n^i(q)\right\}D\left\{Ra(q)\right\}}}. \quad (4)$$

The energy ratio-roughness correlations r_n^i of different frequency bands in each channel are obtained. The channel with the largest energy ratio-roughness correlation in i frequency bands is selected as the sensitive channel, and the other channels with little correlation with surface roughness are eliminated.

4) Wavelet packet fusion reconstruction. Wavelet packet fusion reconstruction is carried out on the wavelet packet coefficients of the sensitive channel. The formula of wavelet packet fusion reconstruction is

$$p_j^i(t)=\sum_{k=1}^{k}h(l-2k)\,p_{j+1}^{2i-1}+\sum_{k=1}^{k}g(l-2k)\,p_{j+1}^{2i}. \quad (5)$$

The multi-channel signal fusion signal is obtained.

1.2 GADF image encoding

Time-domain and time-frequency-domain statistical features can partially capture variations in surface roughness during the machining process. However, manually extracted features may lead to the omission of crucial signal information, while utilizing only time-domain signals restricts the deep learning network model from fully exploiting the interdependencies among data. The utilization of GADF image encoding in this study presents a viable solution to the aforementioned issue[20]. This approach effectively preserves the timing information of the time-domain signal, while also enabling accurate representation of vibration signal amplitude changes through feature maps generated by GADF encoding[21]. Consequently, it facilitates a more comprehensive characterization of surface roughness.

GADF image encoding converts the time and magnitude corresponding to a point of a one-dimensional time series to radius and angle in polar coordinates, transforming the data from one-dimensional to two-dimensional space and generating the Gramian angular difference field based on the sinusoidal function. The process is as follows.

Step 1 The one-dimensional vibration signal sequence $X=\{x_1,x_2,x_3,\cdots,x_n\}$ is scaled to the interval $[-1,1]$ by

$$\tilde{x}_i=\frac{[x_i-\max X]+[x_i-\min X]}{\max X-\min X}, \quad (6)$$

where X represents the amplitude value of the one-dimensional vibration signal; x_i represents the ith amplitude value.

Step 2 The value of the scaled sequence $\tilde{x}_i$ is mapped to the angle θ, while the time is mapped to r, i.e.,

$$\begin{cases}\theta=\arccos\tilde{x}_i, & -1\leqslant\tilde{x}_i\leqslant 1,\tilde{x}_i\in\tilde{X},\\ r=\dfrac{t_i}{N}, & t_i\in N,\end{cases} \quad (7)$$

where t_i represents the time stamp; the interval $[0,1]$ is divided into n equal parts; N represents the constant factor for regulating the radial span of polar coordinates; $\tilde{X}$ represents the normalised time series.

According to Eq. (7), since the scaling range of data is $[-1,1]$, the angle range after conversion is $[0,\pi]$, and the cosine function is monotonic in the interval $[0,\pi]$, which makes a given time series have a unique value in polar coordinates.

Step 3 The Gram angle difference matrix is generated by the operation of trigonometric function difference, i.e.,

$$\boldsymbol{G}_D=\begin{bmatrix}\sin(\theta_1-\theta_1) & \cdots & \sin(\theta_1-\theta_n)\\ \vdots & \vdots & \vdots\\ \sin(\theta_n-\theta_1) & \cdots & \sin(\theta_n-\theta_n)\end{bmatrix}. \quad (8)$$

Step 4 Each element within the matrix is scaled to a value ranging from 0 to 255, corresponding to the pixel size in the image. Subsequently, the GADF image encoding is completed.

1.3 Construction of MA-ResNet model

1.3.1 Multi-scale attention module

Dilated convolution is to inject cavities into the standard convolution kernel. Compared with the pooling layer added after ordinary convolution, which causes part of the information loss. It can increase the receptive field of the model without loss or increase of network parameters[22], and capture information of a larger image range. The basic principle of dilation convolution is to achieve an increase in the sensory field by inserting $r-1$ values with zero weights between the neighboring weights of each row and column of the ordinary convolution, where r is the dilation factor. The calculation formula is

$$F_i=F_{i-1}+(k_i-1)r_i\prod_{n=1}^{i-1}s_n, \quad (9)$$

where F_i represents the sensory field of the convolution kernel in the ith convolutional layer; k_i represents the size of the convolution kernel; r_i represents the dilation

factor; F_{i-1} represents the sensory field of the convolution kernel in the $(i-1)$th convolutional layer; s_n represents the convolutional step size. The schematics of standard and extended convolution are shown in Fig.3.

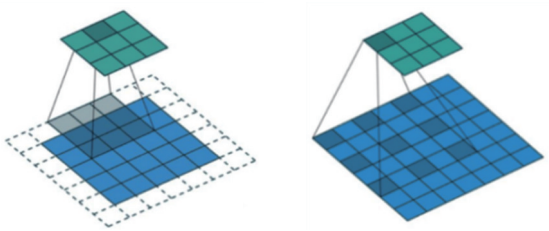

(a) Standard convolution (b) Dilation convolution

Fig. 3 Schematic diagram of standard convolution and dilation convolution

During high-precision machining, the change in vibration signal corresponding to the change in surface roughness is weak. How to effectively capture it is important to improve the prediction accuracy. In order to better capture such weak variations, a multi-scale attention module was proposed. It was composed of two parts: parallel dilation convolution and channel attention mechanism.

First, the extended convolution of four different expansion rates is connected in parallel. The convolution of smaller expansion rate can be used to extract local features, and the convolution of larger expansion rate can be used to extract features between sampling points that are far apart in the time interval, realizing multi-scale feature extraction and avoiding the problem of incomplete representation of single-scale feature information. Then, the obtained multi-scale features are assigned weights through the channel attention mechanism to learn the weights of different scale features[23]. The obtained weights are used to highlight key features and suppress features that are not important for predicting surface roughness, thus helping to identify weak variations. As shown in Fig. 4, a multi-scale attention module is proposed.

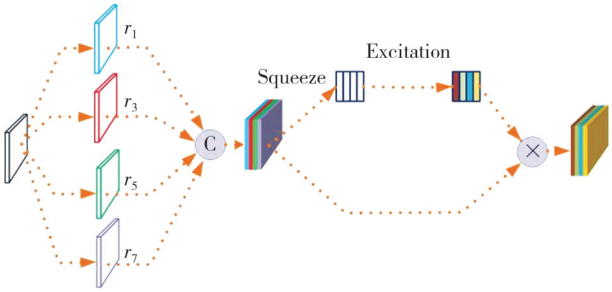

Fig. 4 Multi-scale attention module

1.3.2 Structure of MA-ResNet model

A new network model, namely MA-ResNet model, was proposed by introducing a multi-scale attention module on the basis of residual network. The structure of the model is shown in Fig.5.

The multi-scale attention module is firstly adopted to ensure the complete expression of information and highlight important features. And then multiple residual modules is introduced to process the feature maps, so that there are more nonlinear layers in the model to differentiate the vibration signal features corresponding to different surface roughness values[24,25]. To obtain more expressive features, global average pooling (GAP) is utilized to condense and merge the extracted features. Additionally, a random deactivation layer is incorporated prior to the fully connected layer to mitigate overfitting issues. Finally, prediction is performed by a regression layer. In Fig. 5, Conv 3×3, 2, 32 indicates that the convolution kernel size is 3×3, the step size is 2, and the number of channels is 32, and batch normalization (BN) and rectified linear unit (Relu) operations are performed before each convolution.

2 Experiment

The experimental data were obtained from the machining process of the centerless lathe. The centerless lathe, as a kind of high-precision surface finishing machining equipment, has been able to achieve a surface roughness of the workpiece ranging from 0.3 μm to 0.7 μm. Given its exceptionally smooth machining process and minimal vibration signal fluctuation, it was chosen as the carrier for this experiment. The evaluation indicators for predicting accuracy included the root mean square error (RMSE), the absolute error mean (MAE), and the coefficient of determination (R^2).

2.1 Experimental condition

A centerless lathe was used to machine a bar of material TC4 with a length of 60 m and a diameter of 8 mm, using a total of four tools of YG8 carbide with a front angle of 2°, a back angle of 5°, a main deflection angle of 90°, and an edge inclination angle of 0°. By analysing the working principle of the centreless lathe, it was found that the front end of the spindle was in direct contact with the cutter plate. It could reflect the mutual vibration between the tool and the workpiece during machining, so two different types of sensors were used to monitor the vibration of the two positions at the front end of the spindle during the cutting process. Sensor 1 was a DYTRAN3333A2 single-axis accelerometer sensor, sensor 2 was a KISTLER8704B25 triaxial acceleration sensor, and the sampling frequency of both sensors was 1 024 Hz.

The specific installation directions of the acceleration sensors in each channel are shown in Table 1.

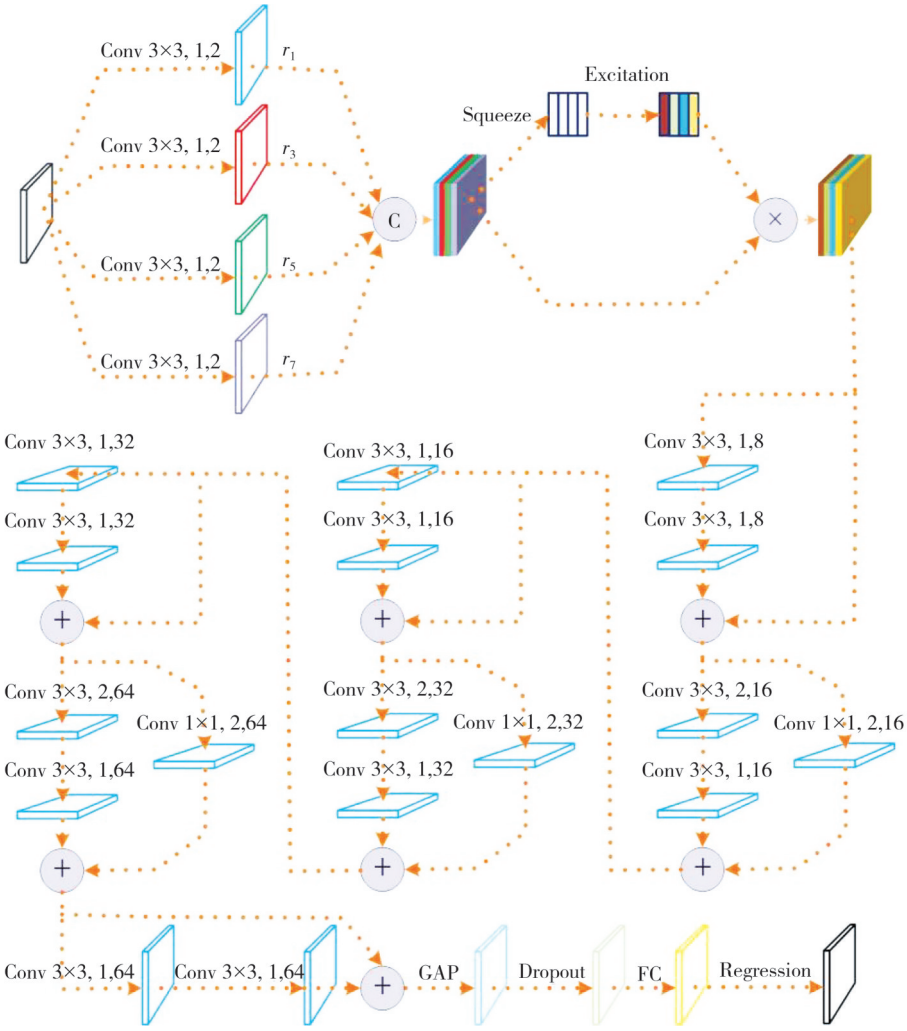

Fig. 5 MA-ResNet model structure diagram

Table 1 Specific mounting orientation of each channel acceleration sensor

Channel	Sensor serial number	Sensor types	Mounting position	Orientations
1	Sensor 1	KISTLER8704B25	Spindle 1	*X*
2	Sensor 2	DYTRAN3333A2	Spindle 2	*X*
3	Sensor 2	DYTRAN3333A2	Spindle 2	*Y*
4	Sensor 2	DYTRAN3333A2	Spindle 2	*Z*

The cutting parameters are set as shown in Table 2.

Table 2 Cutting parameters of TC4 machining process

Level	Spindle speed/(r•min^{-1})	Feed rate/(m•min^{-1})
1	370	0.5
2	420	0.8
3	450	1.0

The machining process covered nine different working conditions, and 30 data collection sessions were conducted under each working condition, obtaining a total of 270 sets of data.

The roughness measuring instrument was TR2000, and the contour arithmetic mean deviation display tages (Ra) was used as the surface roughness measure, and the average value of Ra at four points on the outer circle of the bar was randomly selected as the segment Ra.

2.2 Multi-channel signal fusion

The sampling points of each signal segment are 1 024 in this paper. The vibration signals are decomposed by three-layer wavelet packet, and db1 is selected as the wavelet basis function to obtain signals in 8 frequency bands. 270 sets of data are used to calculate the correlation between energy ratio and roughness of different channels in different frequency bands. The magnitude of the values is shown in Table 3. The channel data with the highest energy ratio-roughness correlation in each frequency band is marked in bold.

It can be found that the energy ratio-roughness correlation of different channels in the same frequency band is obviously different. In order to improve the effective information in the signal, the channel with the largest energy ratio-roughness correlation in the same frequency band is selected as the sensitive channel, and other information is eliminated as redundant information.

Wherein the first frequency band selects the channel

1, the second frequency band selects the channel 2, the third frequency band selects the channel 2, the fourth frequency band selects the channel 2, the fifth frequency band selects the channel 1, the sixth frequency band selects the channel 1, the seventh frequency band selects the channel 4, the eighth frequency band selects the channel 1, and the wavelet packet fusion reconstruction is performed on the screened out sensitive channels to obtain the signal after the fusion of the multi-channels.

Table 3 Energy ratio - roughness correlation of different frequency bands for each channel

Frequency bands	Channel 1	Channel 2	Channel 3	Channel 4
1	**0.440 8**	0.020 9	0.034 2	0.075 4
2	0.243 6	**0.332 1**	0.120 3	0.207 0
3	0.009 1	**0.135 0**	0.047 1	0.003 1
4	0.023 4	**0.135 2**	0.062 2	0.013 2
5	**0.137 8**	0.002 5	0.043 3	0.064 7
6	**0.217 9**	0.069 7	0.130 7	0.152 3
7	0.150 2	0.020 7	0.009 68	**0.198 0**
8	**0.292 8**	0.161 8	0.120 3	0.129 8

2.3 GADF image encoding

The fused signals were encoded in GADF images and then the resolution of each image was adjusted to 128×128 as network input. The *Ra* are 0.397, 0.431, 0.493, 0.593, and 0.643 as well as the corresponding inputs (GADF images of vibration signals after fusion of multi-channel signals), as shown in Fig.6.

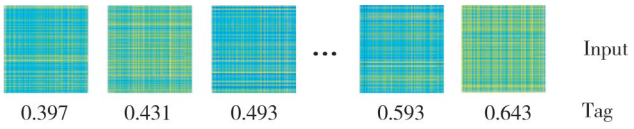

Fig. 6 GADF image encoding after multichannel signal fusion

2.4 Model parameter design

The deep learning framework is deep learning toolbox. After the network structure is determined, the network training uses Sgdm optimizer to optimize the network parameters. The maximum number of training rounds is set to 2 000. The learning rate, as an important hyper-parameter in the deep learning model, determines whether the loss function can converge and when it will converge to the minimum value[26]. In this experiment, the learning rates of 0.003, 0.006, 0.009, 0.012 are used to test the network.

Finally the results trained by different learning rates are compared, and the prediction accuracy is the highest when the learning rate is 0.006. The dropout layer discard rate is set to 0.5 in the network model, which can effectively prevent the overfitting problem. When the loss on the validation set reaches 10 rounds of training and no longer decreases, the training of the network is stopped.

3 Results and discussion

In order to verify the effectiveness of the method proposed in this paper, a comparison experiment between the method of this paper and other methods was conducted. A total of 270 sets of data samples are used in this paper, of which 250 are randomly selected for model training and 20 for testing.

3.1 Comparison of multi-channel signal fusion methods with single-channel signal methods

The commonly used method is single-channel signal. In order to verify the superiority of multi-channel signal fusion proposed in this paper, the single-channel signal and the signal after multi-channel fusion were selected for comparison. The prediction accuracy is shown in Table 4.

Table 4 Prediction accuracy of multi-channel signal fusion and single-channel signal methods

Scheme	Network model	Input type	RMSE	MAE	R^2
1	MA-ResNet	Multi-channel fusion+GADF	0.018 7	0.014 3	0.869 4
2	MA-ResNet	Channel 1+GADF	0.023 3	0.018 4	0.798 2
3	MA-ResNet	Channel 2+GADF	0.024 7	0.020 0	0.772 6
4	MA-ResNet	Channel 3 +GADF	0.027 9	0.022 4	0.711 0
5	MA-ResNet	Channel 4 +GADF	0.025 8	0.021 5	0.751 8

By comparing scheme 1, scheme 2, scheme 3, scheme 4, and scheme 5, it can be found that the highest accuracy of surface roughness prediction based on single channel method is channel 1, in which the RMSE is 0.023 3, MAE is 0.018 4, and R^2 is 0.798 2. These values are obviously lower than the prediction accuracy after multi-channel signal fusion. The reason is that the single-channel signal does not reflect the machine tool state comprehensively during the machining process, while the multi-channel signal fusion method retains more useful information while eliminating the redundant information that has little correlation with the surface roughness, thus further improving the prediction accuracy. Moreover, the model test set takes 1 s and contains a total of 20 experimental data. Therefore, the time of processing a single use case is as low as 50 ms, reaching the millisecond level, which meets the real-time requirement of online prediction of surface roughness. The comparison of the prediction curves and absolute errors for scenarios 1 and 2 are shown in Fig.7.

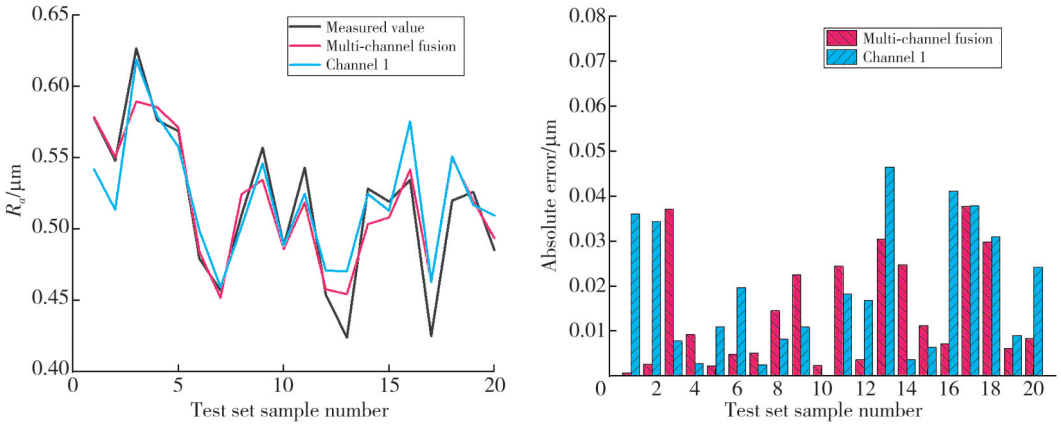

(a) Projection curve (b) Absolute error comparison chart

Fig. 7 Comparison of prediction curves and absolute errors between channel 1 and multi-channel fusion methods

3.2 Comparison of different image encoding methods

Image encoding helps deep learning models make better use of the correlation between data. In this paper, image encoded by GADF, GASF, and MTF are respectively used as inputs to study the influence of different encoding methods on prediction accuracy. The prediction accuracy of different image codes is shown in Table 5.

Table 5 Prediction accuracy of different encoding methods

Scheme	Network model	Input type	RMSE	MAE	R^2
1	MA-ResNet	Multi-channel fusion+GADF	0.018 7	0.014 3	0.869 4
2	MA-ResNet	Multi-channel fusion+GASF	0.021 2	0.016 5	0.833 2
3	MA-ResNet	Multi-channel fusion+MTF	0.022 4	0.017 6	0.814 0

By comparing scheme 1, scheme 2, and scheme 3, it can be seen that the GADF image encoding method has a higher prediction accuracy than the other two image encoding methods, and therefore it can be proved that the image encoding method of GADF is more suitable for the expression of the relevant roughness features in the vibration signals compared with the other two methods. The prediction curves and absolute error comparison graphs of the three schemes are shown in Fig.8.

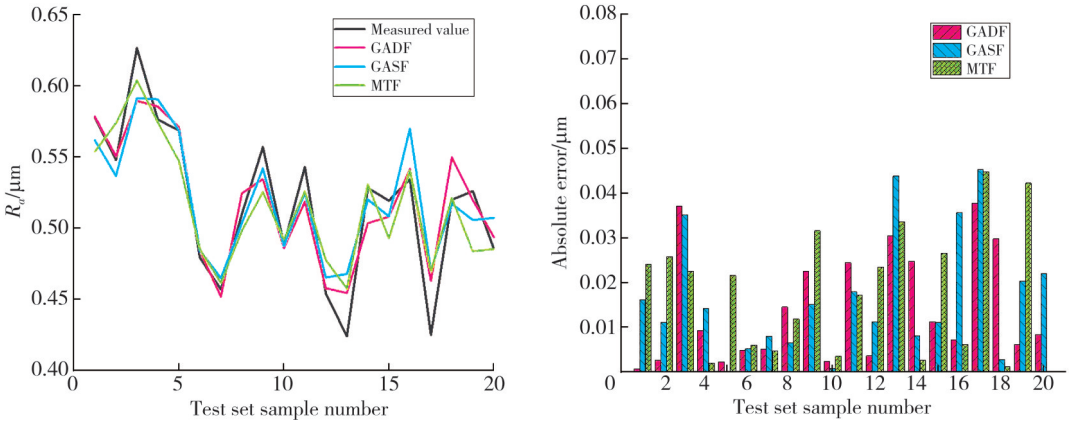

(a) Projection curve (b) Absolute error comparison chart

Fig. 8 Comparison of prediction curves and absolute errors of different image encoding

3.3 Comparison with different network models

GADF with multi-channel signal fusion was used as input, and two methods, ResNet and CNN (convolutional neural network), were added for comparison experiments. Among them, ResNet used MA-ResNet with the multi-scale attention module removed. The prediction accuracy of different network models is shown in Table 6.

By comparing scheme 1, scheme 2, and scheme 3, it can be clearly seen that MA-ResNet has the highest prediction accuracy compared with the other two networks, followed by ResNet, and CNN has the lowest prediction accuracy. The reason is that MA-ResNet employs a multi-scale attention module, which

enables the model to highlight important features while ensuring the complete expression of information, and avoids the difficulty of identifying weak differences in the data signals due to the small changes in the data signals themselves, thus realizing the prediction of surface roughness for high-precision machining. The prediction curves and absolute error comparison figures of the three schemes are shown in Fig.9.

Table 6 Prediction accuracy of different network models

Scheme	Network model	Input type	RMSE	MAE	R^2
1	MA-ResNet	Multi-channel fusion+GADF	0.018 7	0.014 3	0.869 4
2	ResNet	Multi-channel fusion+GADF	0.026 5	0.020 8	0.739 5
3	CNN	Multi-channel fusion+GADF	0.028 4	0.023 2	0.700 0

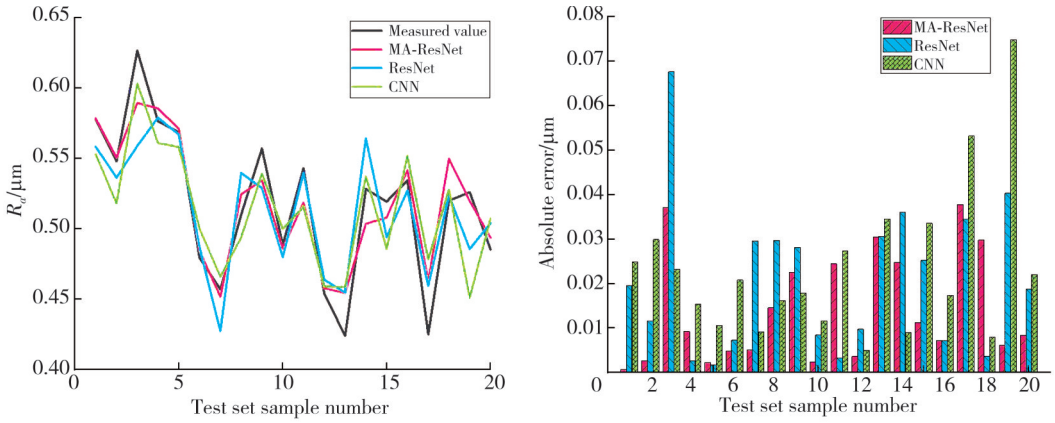

(a) Projection curve (b) Absolute error comparison chart

Fig. 9 Comparison of prediction curves and absolute errors for different network models

4 Conclusions

An input layer construction method of GADF prediction model based on multi-channel signal fusion was proposed. Firstly, the multichannel signals were screened and fused to eliminate the information that had little relevance to the predicted target. Then the fused signals were converted into GADF images, so that the inputs were converted into a form that was easy to reflect the characteristics of the target, which improved the accuracy of the prediction model. This method had reference value for constructing the input form of surface roughness prediction model.

Multi-scale dilation convolution and attention mechanism were combined on the basis of residual network, so that the model could ensure the complete expression of information while highlighting important features, and avoid the difficulty in identifying weak differences due to the slight changes of the data signal itself, so as to achieve the surface roughness prediction of high-precision machining. The results showed that the proposed method was of good engineering significance for high-precision prediction, which was conducive to the on-line monitoring of the surface quality of the workpiece machining process.

Acknowledgement

This work was supported by Shaanxi Province Key Research and Development Plan (No. 2023-YBGY-386) and Shaanxi Province Key Research and Development Plan (No.2022-JBGS-07).

Declaration of conflicting interests

The authors have no conflict of interests related to this publication.

References

[1] HE B F, DING S Y, WEI C E, et al. Review of measurement methods for areal surface roughness. Optics and Precision Engineering, 2019, 27(1): 78-93.

[2] WEI W Z, TIAN J Y, JIANG Q, et al. Support vector machine detection model of part surface roughness based on image technology. Modern Manufacturing Engineering, 2022(5): 100-109.

[3] FAN Z L. Research on surface roughness detection method of slender parts based on machine vision. Hangzhou: Zhejiang University of Science and Technology, 2021.

[4] GIUSTI A, DOTTA M, MARADIA U, et al. Image-based measurement of material roughness using machine learning techniques. Procedia CIRP, 2020, 95: 377-382.

[5] MIN L, WANG Z, DONG S. Surface roughness detection of end milling based on Hough transform and GLCM.

Control Engineering, 2019, 26(4): 645-651.

[6] YANG A M, HAN Y, PAN Y H, et al. Optimum surface roughness prediction for titanium alloy by adopting response surface methodology. Results in Physics, 2017, 7: 1046-1050.

[7] LIU H J, YANG S X. Roughness modeling method based on improved particle swarm neural network. Modular Machine Tool & Automatic Manufacturing Technique, 2018(6): 62-64.

[8] WANG X M, HAN J. Research on surface roughness of TC4 titanium alloy high speed milling. Mechanical Design and Manufacturing, 2019(5): 232-236.

[9] SHI L C, JIA Y K, ZHANG J F. Research on technological parameters of removing oxide coating from titanium alloy bar surface by turning. Surface Technology, 2021, 50(5): 372-379.

[10] PENG B B, YAN X G, DU J. Surface quality prediction based on BP and RBF neural networks. Surface Technology, 2019, 49(10): 324-328.

[11] CHI J, CHEN L Q, YANG C Z. Reasearch on prediction of cutting surface roughness based on wavelet packet analysis and Elman network. China Mechanical Engineering, 2010, 21(7): 822-826.

[12] GARCÍA PLAZA E, NÚÑEZ LÓPEZ P J. Surface roughness monitoring by singular spectrum analysis of vibration signals. Mechanical Systems and Signal Processing, 2017, 84: 516-530.

[13] ZHU J J, PU Y, ZHOU R G. Surface roughness prediction based on feature sorting neural network algorithm. Computer Integrated Manufacturing System, 2020, 26 (12): 3268-3273.

[14] TAN F F, ZHU J J, YAN T H, et al. Prediction of surface roughness of 6061 aluminum alloy based on GA-WPT-ELM. Journal of Zhejiang University (Engineering Edition), 2020, 54(1): 40-47.

[15] LIN W J, LO S H, YOUNG H T, et al. Evaluation of deep learning neural networks for surface roughness prediction using vibration signal analysis. Applied Sciences, 2019, 9(7): 1462.

[16] PAN Y N, KANG R K, DONG Z G, et al. On-line prediction of ultrasonic elliptical vibration cutting surface roughness of tungsten heavy alloy based on deep learning. Journal of Intelligent Manufacturing, 2022, 33(3): 675-685.

[17] SHI L C, YYANG P D, WANG H T. Surface roughness prediction based on Wavelet packet transform-residual network. Computer Integrated Manufacturing Systems, 2019, 29(10): 3249-3257.

[18] HOU Z G, WANG H W, XIONG M L, et al. Gearbox fault diagnosis based on transfer learning and weighted multi-channel fusion. Journal of Vibration and Shock, 2023, 42(9): 236-246.

[19] ZHANG Z, JIA Z T. Fault line selection method based on wavelet packet decomposition and residual network. Computer Simulation, 2023, 40(3): 110-115.

[20] TONG Y, PANG X Y, WEI Z H. Fault diagnosis method of rolling bearing based on GADF-CNN. Journal of Vibration and Shock, 2021, 40(5): 247-253.

[21] PAN Y S, QIN C. Identification method for distribution network topology based on two-stage feature selection and gramian angular field. Automation of Electric Power Systems, 2022, 46(16): 170-177.

[22] LI K Y, ZHU X Y, MA J C, et al. Estimation of cucumber disease severity based on mixed expansionconvolution and attention. Journal of Agricultural Machinery, 2023, 54 (2): 231-239.

[23] ZHANG Y F, YI Y H, TANG Z W, et al. Text-to-image synthesis method based on channel attention mechanism. Computer Engineering, 2022, 48(4): 206-212.

[24] WANG D F, SU H S, CHEN D K, et al. A method of railway fastener defect detection based on Res Nt-SSDe. Journal of Measurement Science and Instrumentation, 2023, 14(3): 360-368.

[25] HU H M, ZHANG L H. Pedestrian attribute recognition based on residual attention and asymmetric loss. Journal of Testing Technology, 2023, 37(2): 99-105.

[26] ZHANG X D, WANG T J, ZHU S J, et al. Hyperspectral image classification based on extended convolutional attention neural networks. Journal of Optics, 2021, 41(3): 49-59.

基于多通道信号融合的GADF与MA-ResNet的车削表面粗糙度预测

史丽晨*, 刘腾飞, 王海涛

西安建筑科技大学 机电工程学院, 陕西 西安 710055

摘　要： 为了实现车削加工过程中表面粗糙度的高精度在线预测，提高切削质量，提出了一种基于多通道信号融合的格拉姆角差场(Gramian angular difference field, GADF)与多尺度注意力残差网络(Multi-scale attention residual networks, MA-ResNet)的车削表面粗糙度预测方法。首先，利用小波包分解将多通道振动信号细分到各个频段，并通过对各频段信号与表面粗糙度做相关分析，选择出敏感通道进行信号融合。然后，将融合后的信号利用格拉姆角差场(GADF)图像编码转换为图片。最后，将图片输入到结合了并行扩张卷积与注意力模块的残差网络模型中进行训练，并验证模型性能的有效性。本文所提方法在预测表面粗糙度时均方根误差为0.018 7，绝对误差平均值为0.014 3，决定系数为0.869 4，预测值与实际值接近。因此，本文所提方法对于高精度预测具有较好的工程意义，有利于工件加工过程中表面质量的在线监测。

关键词： 信号融合；格拉姆角差场；扩张卷积；残差网络；粗糙度预测

引用格式： SHI Lichen, LIU Tengfei, WANG Haitao. Prediction of turned surface roughness based on GADF of multi-channel signal fusion and MA-ResNet. Journal of Measurement Science and Instrumentation, 2025, 16(2): 302-312. DOI: 10.62756/jmsi.1674-8042.2025029